

Comparative Isotropic Shifts, Redox Potentials, and Ligand Binding Propensities of [1:3] Site-Differentiated Cubane-Type $[\text{Fe}_4\text{Q}_4]^{2+}$ Clusters (Q = S, Se)

Chaoyin Zhou and R. H. Holm*

Department of Chemistry and Chemical Biology, Harvard University, Cambridge, Massachusetts 02138

Received March 4, 1997[⊗]

The [1:3] site-differentiated cubane-type clusters $[\text{Fe}_4\text{Q}_4(\text{LS}_3)\text{Cl}]^{2-}$ (Q = S, Se; $\text{LS}_3 = 1,3,5\text{-tris}((4,6\text{-dimethyl-3-mercaptophenyl})\text{thio})\text{-}2,4,6\text{-tris}(p\text{-tolylthio})\text{benzenate}(3-)$) undergo substitution reactions at the unique iron site with a variety of ligands including thiolates, phenolates, cyclic triamines and a trisulfide, imidazoles, and tertiary phosphines. Reactions are readily followed because of the extreme sensitivity of isotropically shifted resonances to the nature of ligand L' in the product clusters $[\text{Fe}_4\text{Q}_4(\text{LS}_3)L']^{2-}$. Isotropic shifts and redox potentials are reported for over 40 clusters, including many cluster pairs differing only in the core chalcogenide atom. In this way, comparative properties of sulfide and selenide clusters can be elicited. It is shown that the larger isotropic shifts consistently observed for selenide clusters and dominantly contact in nature arise from larger magnetic susceptibilities, which indicate a lesser extent of antiferromagnetic coupling. It is further demonstrated that, without exception, redox potentials of selenide clusters are more positive than those of sulfide clusters, usually by 20–60 mV, at parity of ligation. The difference in potentials of *ca.* 300 mV between the $[\text{Fe}_4\text{S}_4]^{2+,+}$ couples of $[\text{Fe}_4\text{S}_4(\text{LS}_3)(\text{SEt})]^{2-}$ and $[\text{Fe}_4\text{S}_4(\text{LS}_3)(\text{Im})]^-$ (Im = imidazole) clusters is the best available estimate of the intrinsic potential difference between protein-bound $[\text{Fe}_4\text{S}_4(\text{Cys-S})_4]$ and $[\text{Fe}_4\text{S}_4(\text{Cys-S})_3(\text{His-N})]$ clusters. The ligand LS_3 undergoes spontaneous transfer between $[\text{Fe}_4\text{S}_4]^{2+}$, $[\text{Fe}_4\text{Se}_4]^{2+}$, and $[\text{MoFe}_3\text{S}_4]^{3+}$ cores in reactions whose equilibrium constants are near the statistical value. The ligand binding affinity order $\text{PhS}^- > \text{PhO}^- > \text{CN}^- \gg \text{Cl}^-$ for $[\text{Fe}_4\text{Q}_4]^{2+}$ cores was established. When taken together with earlier results from this laboratory, a comprehensive picture of ligand binding to single iron sites in $[\text{Fe}_4\text{Q}_4]^{2+}$ clusters emerges.

Introduction

The synthesis and development of the chemistry of cubane-type Fe_4S_4 clusters in which one iron site is differentiated from the other three by terminal ligation¹ has been motivated by the occurrence of related [1:3] site-differentiated clusters in proteins. In this context, the $[\text{Fe}_4\text{S}_4(\text{Cys-S})_3(\text{OH}_2/\text{OH})]$ active site of aconitase has been demonstrated crystallographically;^{2,3} its unique iron atom is the site of the hydration–dehydration reaction sequence of the enzyme and of inhibitor binding.³ It is highly probable that other hydrolyases have analogous catalytic sites.⁴ Further, the catalytic center of *Escherichia coli* sulfite reductase is now known to consist of a $[\text{Fe}_4\text{S}_4(\text{Cys-S})_3(\mu\text{-Cys-S})]$ cluster bridged to a siroheme group, at which substrate is bound and reduced.⁵ Current evidence points to the existence of coupled $[\text{Fe}_4\text{S}_4(\text{Cys-S})_3\text{-X-Ni}]$ units (bridging group X unidentified) at both catalytic nickel centers of the carbon monoxide dehydrogenase from *Clostridium thermoaceticum*.^{6,7}

Our approach to [1:3] site-differentiated Fe_4Q_4 clusters has utilized species of the type $[\text{Fe}_4\text{Q}_4(\text{LS}_3)L']^{2-}$ with Q = S (1^{S}) or Se (1^{Se}), depicted in Figure 1. The semirigid trithiolate cavitand ligand LS_3 ⁸ binds the cluster in a trigonally symmetric arrangement, engendering regiospecific reactivity at the unique

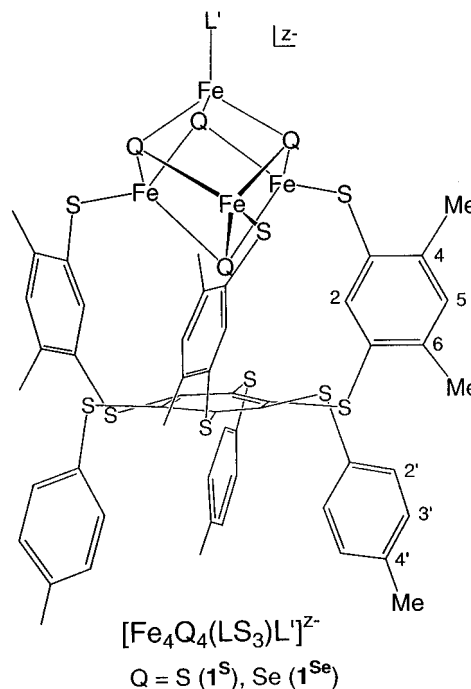


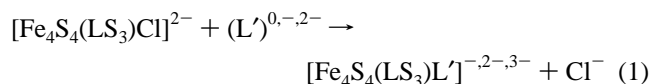
Figure 1. Schematic structure of the [1:3] site-differentiated clusters $[\text{Fe}_4\text{Q}_4(\text{LS}_3)L']^{2-}$ (Q = S, Se). The numbering scheme for substituents on the coordinating “arms” and buttressing “legs” of the LS_3 ligand system is indicated.

iron site. This binding mode has been established by X-ray structures of two $[\text{Fe}_4\text{Q}_4(\text{LS}_3)\text{Cl}]^{2-}$ clusters⁸ and is otherwise entirely consistent with the isotropically shifted ^1H NMR spectra, which without exception disclose trigonal symmetry. Applications of the $\text{Fe}_4\text{S}_4(\text{LS}_3)$ system include formation of bridged double cubanes with redox reactions coupled across bridges of variable length,⁹ generation of five- and six-coordinate iron sites with attendant modulation of cluster charge distribution, redox

[⊗] Abstract published in *Advance ACS Abstracts*, August 15, 1997.

- (1) Holm, R. H.; Ciurli, S.; Weigel, J. A. *Prog. Inorg. Chem.* **1990**, *29*, 1.
- (2) Robbins, A. H.; Stout, C. D. *Proc. Natl. Acad. Sci. U.S.A.* **1989**, *86*, 3639.
- (3) Beinert, H.; Kennedy, M. C.; Stout, C. D. *Chem. Rev.* **1996**, *96*, 2335.
- (4) Flint, D. H.; Allen, R. M. *Chem. Rev.* **1996**, *96*, 2315.
- (5) Crane, B. R.; Siegel, L. M.; Getzoff, E. D. *Science* **1995**, *270*, 59.
- (6) Ragsdale, S. W.; Kumar, M. *Chem. Rev.* **1996**, *96*, 2515.
- (7) (a) Xia, J.; Lindahl, P. A. *J. Am. Chem. Soc.* **1996**, *118*, 483. (b) Hu, Z.; Spangler, N. J.; Anderson, M. E.; Xia, J.; Ludden, P. W.; Lindahl, P. A.; Münck, E. *J. Am. Chem. Soc.* **1996**, *118*, 830.
- (8) (a) Stack, T. D. P.; Holm, R. H. *J. Am. Chem. Soc.* **1988**, *110*, 2484. (b) Stack, T. D. P.; Weigel, J. A.; Holm, R. H. *Inorg. Chem.* **1990**, *29*, 3745.

potentials, and spin state,^{10,11} formation of sulfide-bridged cluster-heme assemblies related to sulfite reductase,¹² and conversion to the cuboidal cluster [Fe₃S₄(LS₃)]³⁻ by removal of the unique iron atom.¹³ Throughout this work, the hypersensitivity of isotropic shifts of the 2-H, 4-Me, 5-H, and 6-Me substituents on the coordinating arms of the LS₃ ligand (Figure 1) to the ligand bound at the unique site has allowed detection of ligand binding in solution. This situation is exemplified by reaction 1,^{10,14} in which the relatively labile chloride ligand is replaceable by a variety of other ligands to afford a unique iron site with coordination number 4, 5, or 6. All [Fe₄S₄]²⁺ clusters have a singlet ground state and a low-lying triplet state, partial occupation of which in both synthetic⁸⁻¹⁴ and native¹⁵ clusters affords isotropic shifts.



Practically all of our previous work on [1:3] site-differentiated clusters has been carried out with species containing the [Fe₄S₄]²⁺ core. Certain iron-sulfur apoproteins have been reconstituted with an iron salt and selenide, affording [Fe₄Se₄]²⁺ clusters, which apparently produce only small changes in protein structure while exhibiting optical and ¹H NMR spectra and redox potentials somewhat perturbed compared to those of native proteins. The consequences of S/Se replacement and the use of selenide as a structural and electronic probe have been well treated by Meyer *et al.*¹⁶ A number of the properties of protein-bound selenide clusters have been anticipated or substantiated by results for [Fe₄Se₄(SR)₄]²⁻ synthetic clusters. They include red-shifted absorption spectra,^{17,18} positively shifted redox potentials,^{17,18} larger ¹H NMR chemical shifts,¹⁸⁻²⁰ and in [Fe₄Se₄(SR)₄]³⁻ clusters a clear tendency to stabilize a ground state spin *S* > 1/2.^{18,20} We have also demonstrated core chalcogenide exchange reactions between [Fe₄Q₄(SR)₄]^{2-/3-} clusters (Q = S, Se) in the same oxidation state, the exchange being much faster between [Fe₄Q₄]⁺ species.²¹ In addition, we have proven the reversible interconversions [Fe₃Q₄]⁰ + Fe²⁺ ⇌ [Fe₄Q₄]²⁺ (Q = S, Se)¹³ as found for aconitase.^{3,22} Further, the [Fe₄Se₄]²⁺ form of aconitase is reported to show a higher activity with isocitrate as substrate than the native [Fe₄S₄]²⁺ form.²² Given the continued interest in and utility of selenide-substituted clusters,¹⁶ several fundamental properties of [Fe₄Se₄]²⁺ clusters, taken relative to [Fe₄S₄]²⁺ clusters, require

further clarification and have not been examined previously. In the present study, we have utilized the clusters **1^S** and **1^{Se}** to scrutinize these aspects of selenide substitution into the core structure: (i) binding of variant ligands at the differentiated site; (ii) the origin of the (usually) larger isotropic shifts of selenide vs sulfide clusters; (iii) patterns of ligand spin density distribution; (iv) dependence of redox potential on variation of ligand L', including the previously unexamined but physiologically relevant case of imidazole ligation; (v) exchange of the LS₃ ligand between sulfide and selenide clusters. In the examination of ligand binding and exchange reactions, (ii) can offer the advantage of increased chemical shift resolution helpful or necessary to product identification. Here we utilize aspect (ii) to investigate intercluster ligand exchange reactions of both L' and LS₃ itself in [Fe₄Q₄(LS₃)L']²⁻ clusters.

Experimental Section²³

Preparation of Compounds. All operations were carried out under a pure dinitrogen atmosphere. Acetonitrile was distilled from CaH₂ and THF from sodium benzophenone ketyl. Deuterated acetonitrile was dried over molecular sieves prior to use. Sodium phenolates and thiolates were obtained by the reaction of NaH with the phenol or thiol in THF. 4,6-Dimethyl-1,3-benzenedithiol,²⁴ Na₂(mnt),²⁵ and [9]aneS₃²⁶ were prepared as described. Li₂Se was prepared by the reaction of Se powder with Li(Et₃BH) in THF.²⁷ All other compounds were commercial samples.

(Bu₄N)₂[Fe₄Se₄(SEt)₄]. This compound is more readily obtained in the pure state and is more soluble than the previously reported Et₄N⁺ salt;¹⁸ it is the precursor to (Bu₄N)₂[Fe₄Se₄(LS₃)(SEt)].¹³ To a solution of 106 mmol of NaOEt in 200 mL of ethanol was added 7.90 mL (106 mmol) of ethanethiol followed by solution of 4.30 g (26.5 mmol) of FeCl₃ in 100 mL of ethanol. The reaction mixture was stirred for 30 min, and 2.09 g (26.5 mmol) of selenide powder was added. Stirring was continued overnight, and the mixture was filtered. A solution of 4.90 g (13.3 mmol) of Bu₄NI in 250 mL of methanol was slowly added to the filtrate with stirring over a period of 10 h. The product was collected by filtration, washed with 300 mL of methanol and then with ether, and dried in vacuo to give 7.15 g (85%) of pure product as a black microcrystalline solid. ¹H NMR (CD₃CN): δ 15.2 (CH₂), 2.68 (CH₃). The spectrum of the anion is identical with that of the Et₄N⁺ salt.¹⁸

(Bu₄N)₂[Fe₄Q₄(LS₃)Cl] (Q = S, Se). To a solution of 0.492 mmol of (Bu₄N)₂[Fe₄Q₄(LS₃)(SEt)] (Q = S,^{12a} Se¹³) in 150 mL of acetonitrile was added 67.8 mg (0.492 mmol) of solid (Et₃NH)Cl. The reaction mixture was stirred for 12 h, during which time it was subjected to dynamic vacuum about every 4 h for 10 min to remove ethanethiol and triethylamine. The reaction mixture was filtered and the solvent removed in vacuo to afford the pure product in essentially quantitative yield. The ¹H NMR spectrum of the Q = S product in CD₃CN solution is identical with that of the Ph₄P⁺ salt in the same solvent.^{8a} ¹H NMR spectrum of [Fe₄Se₄(LS₃)Cl]²⁻ (CD₃CN): δ 8.52 (5-H), 7.03 (2'-H), 6.64 (3'-H), 5.52 (2-H), 4.38 (4-Me), 3.96 (6-Me), 2.21 (4'-Me).

Generation of Clusters in Solution. To a solution of (Bu₄N)₂[Fe₄Q₄(LS₃)Cl] (Q = S, Se) in acetonitrile was added 1 equiv of a solution of sodium thiolate in acetonitrile or a solution of sodium phenolate in 1:1 acetonitrile/methanol (v/v). Cyanide-ligated clusters were generated with 1 equiv of (Et₄N)(CN) in acetonitrile. The acetate-ligated cluster was formed by the reaction of equimolar [Fe₄Se₄(LS₃)(OC₆H₄-*p*-Br)]²⁻ and Me₃SiOAc in acetonitrile. With neutral ligands, a solution of 3 or more equiv in acetonitrile was added together

- (9) Stack, T. D. P.; Carney, M. J.; Holm, R. H. *J. Am. Chem. Soc.* **1989**, *111*, 1670.
 (10) Ciurli, S.; Carrié, M.; Weigel, J. A.; Carney, M. J.; Stack, T. D. P.; Papaefthymiou, G. C.; Holm, R. H. *J. Am. Chem. Soc.* **1990**, *112*, 2654.
 (11) Weigel, J. A.; Srivastava, K. K. P.; Day, E. P.; Münck, E.; Holm, R. H. *J. Am. Chem. Soc.* **1990**, *112*, 8015.
 (12) (a) Cai, L.; Holm, R. H. *J. Am. Chem. Soc.* **1994**, *116*, 7177. (b) Zhou, C.; Cai, L.; Holm, R. H. *Inorg. Chem.* **1996**, *35*, 2767.
 (13) Zhou, J.; Hu, Z.; Münck, E.; Holm, R. H. *J. Am. Chem. Soc.* **1996**, *118*, 1966.
 (14) Weigel, J. A.; Holm, R. H. *J. Am. Chem. Soc.* **1991**, *113*, 4184.
 (15) (a) Bertini, I.; Turano, P.; Vila, A. J. *Chem. Rev.* **1993**, *93*, 2833. (b) Bertini, I.; Ciurli, S.; Luchinat, C. *Struct. Bonding* (Berlin) **1995**, *83*, 1.
 (16) Meyer, J.; Moulis, J.-M.; Gaillard, J.; Lutz, M. *Adv. Inorg. Chem.* **1992**, *38*, 73.
 (17) Bobrik, M. A.; Laskowski, E. J.; Johnson, R. W.; Gillum, W. O.; Berg, J. M.; Hodgson, K. O.; Holm, R. H. *Inorg. Chem.* **1978**, *17*, 1402.
 (18) Yu, S.-B.; Papaefthymiou, G. C.; Holm, R. H. *Inorg. Chem.* **1991**, *30*, 3476.
 (19) Reynolds, J. G.; Coyle, C. L.; Holm, R. H. *J. Am. Chem. Soc.* **1980**, *102*, 4350.
 (20) Carney, M. J.; Papaefthymiou, G. C.; Whitener, M. A.; Spartalian, K.; Frankel, R. B.; Holm, R. H. *Inorg. Chem.* **1988**, *27*, 346.
 (21) Reynolds, J. G.; Holm, R. H. *Inorg. Chem.* **1981**, *20*, 1873.
 (22) Surerus, K. K.; Kennedy, M. C.; Beinert, H.; Münck, E. *Proc. Natl. Acad. Sci. U.S.A.* **1989**, *86*, 9846.

- (23) Abbreviations: [9]aneS₃, 1,4,7-trithiacyclononane; [9]aneS₃O, 1,4,7-trithiacyclononane S-oxide; Clacat, tetrachlorocatecholate(2-), Fe, ferrocene; Im, imidazole; LS₃, 1,3,5-tris(4,6-dimethyl-3-mercaptophenyl)thio)-2,4,6-tris(*p*-tolylthio)benzenate(3-); Meida, (methylimino)diacetate(2-); mnt, maleonitriledithiolate(2-); tacn, 1,4,7-triazacyclononane.
 (24) (a) Wagner, A. W. *Chem. Ber.* **1966**, *99*, 375. (b) Morgenstern, J.; Mayer, R. Z. *Chem.* **1968**, *8*, 106.
 (25) Davison, A.; Holm, R. H. *Inorg. Synth.* **1967**, *10*, 8.
 (26) Blower, P. J.; Cooper, S. R. *Inorg. Chem.* **1987**, *26*, 2009.
 (27) Gladysz, J. A.; Hornby, J. L.; Garbe, J. E. *J. Org. Chem.* **1978**, *43*, 1204.

Table 1. Crystallographic Data for (Bu₄N)[Fe₄Se₄(LS₃)([9]aneS₃)]·[9]aneS₃

formula	C ₇₈ H ₁₀₃ Fe ₄ NS ₁₅ Se ₄
fw	2074.75
cryst system	orthorhombic
space group	<i>P</i> 2 ₁ 2 ₁ 2 ₁
<i>Z</i>	4
<i>a</i> , Å	16.5445(1)
<i>b</i> , Å	20.2188(3)
<i>c</i> , Å	26.7010(5)
<i>V</i> , Å ³	8931.8(2)
ρ_{calcd} , g/cm ³	1.543
μ , cm ⁻¹	2.66
λ , Å	0.710 73
<i>T</i> , °C	-60
<i>R</i> ₁ , ^a <i>wR</i> ₂ ^b	0.0838, 0.1679

$$^a R_1 = \sum ||F_o| - |F_c|| / \sum |F_o|. \quad ^b wR_2 = \{ \sum [w(F_o^2 - F_c^2)^2] / \sum [w(F_o^2)^2] \}^{1/2}$$

with a solution of 4 equiv of NaBF₄ in methanol. Reaction solutions were stirred for 1–2 h at ambient temperature and volatile components removed *in vacuo*. The cluster salts and, when present, free ligands were dissolved in a suitable volume of acetonitrile for examination by ¹H NMR spectroscopy and voltammetry. Solvent volumes were chosen to give *ca.* 2 mM cluster solutions. Residual salts are essentially insoluble (NaCl) or sparingly soluble (NaBF₄) in acetonitrile. The NMR spectra indicated a >95% conversion to the substituted cluster product; no other cluster species were detected in these spectra. Ratios of neutral ligands and clusters were employed which gave limiting NMR spectra and *E*_{1/2} values (±10 mV) upon the addition of a further excess of ligand.

Equilibrium Constants. In LS₃ ligand exchange reactions, equimolar (*ca.* 2 mM) solutions of the starting clusters in acetonitrile solutions were mixed and stirred, and the reactions monitored by ¹H NMR until equilibrium was reached. In the study of preferential ligand binding in acetonitrile, a stock solution equimolar in (Et₄N)(CN), (Bu₄N)(OPh), and (Bu₄N)(SPh) was added to a solution of 2 mM [Fe₄Q₄(LS₃)Cl]²⁻ (Q = S, Se) such that there was initially 0.5 equiv of free ligand per cluster. The mixtures were stirred for 1 h and the NMR spectra recorded. Equilibrium constants were calculated from integrated signals of 4-Me, 5-H, 6-Me, 2'-H, and 3'-H, as appropriate.

X-ray Structure Determination. Intensity data were collected on a Siemens SMART CCD diffractometer equipped with an LT-2 low-temperature apparatus operating at 213 K. Black crystals of (marginal) diffraction quality were grown from ~10 mM solutions (containing excess ligand) in acetonitrile. A crystal was mounted on a glass fiber. Data were measured using Ω scans of 0.3 Å per frame for 60 s, such that a hemisphere was collected. A total of 1271 frames was collected with a final resolution of 0.90 Å. No intensity decay was observed over the period of data collection. Cell parameters were obtained using SMART software (Siemens Analytical Instruments, Madison, WI) and were refined using SAINT on all observed reflections. Crystal data are given in Table 1. Data reduction was performed with SAINT; absorption corrections were applied with SADABS. The structure was solved by direct methods using the SHELXS-90 program and was refined by least-squares methods with SHELXTL-93. The space group was established by analysis of systematic absences, *E* statistics, and successful refinement of the structure. The asymmetric unit consists of one cation, one anion, and one molecule of [9]aneS₃. All non-hydrogen atoms were described anisotropically. Hydrogen atoms were assigned to ideal positions and refined using a riding model with isotropic thermal parameters 1.2× or 1.5× (methyl groups) those of the attached carbon atoms.²⁸

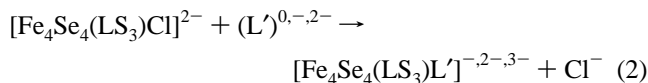
Other Physical Measurements. All measurements were performed under strictly anaerobic conditions. ¹H NMR spectra were obtained at 297 K using a Bruker AM-500 spectrometer. Electrochemical measurements were made with standard PAR instrumentation in acetonitrile solutions with 0.1 M (Bu₄N)(PF₆) supporting electrolyte, a Pt working electrode, and an SCE reference electrode. Cyclic voltammograms were recorded at a scan rate of 20 mV/s. Under these conditions, *E*_{1/2}(Fc⁺/Fc) = +0.39 V. Magnetic measurements in solution were made by the standard ¹H NMR method²⁹ using Me₄Si as the reference compound.

(28) See paragraph at the end of this article concerning Supporting Information available.

Results and Discussion

Clusters 2–31, listed in Tables 2 and 3, are of principal interest in this investigation. The set includes some 13 pairs of clusters differing only in the core Q atom (e.g., 2^S/2^{Se} in Table 2) for which one or both of the comparative properties of isotropically shifted NMR spectra and redox potentials have been determined. The structures of the clusters are schematically depicted in Figure 2.

Scope of Ligand Substitution. Previously, we have reported the occurrence of reaction 1 with sulfide cluster 2^S in Me₂SO solution with a large range of ligands L', and have described the response of ¹H NMR isotropic shifts and redox potentials to variation in ligand at the unique iron site.^{1,8a,9–14,30} Here we have examined the analogous ligand substitution reaction 2 of



selenide cluster S^{Se} in acetonitrile solution. This solvent was chosen because of the less robust nature of the [Fe₄Se₄]²⁺ core but particularly to minimize competition between the binding of solvent and added neutral ligands in reactions with both 2^S and 2^{Se}. The reactions summarized in Figure 2 were conducted *in situ* at ambient temperature and were monitored by ¹H NMR spectroscopy. Selenide clusters were generated in this way, while the smaller set of sulfide clusters was obtained by reaction 1. Among the former are 5^{Se} and 19^{Se}, whose NMR spectra are compared with those of their sulfide analogues in Figures 3 and 4, respectively. These are the first comparative spectra published for [Fe₄Q₄]²⁺ clusters and immediately reveal the enhanced downfield chemical shifts of selenide clusters.³¹ It is the isotropic shifts, compiled in Tables 2 and 3, that are responsible for differences between the sulfide and selenide clusters. Of the most shifted resonances in the 5^S/5^{Se} pair, the methylene protons experience a 22% larger isotropic shift in the selenide cluster. Similarly, in the 19^S/19^{Se} pair, the 4-Me shift in the selenide cluster is 32% larger. These factors are not uniform for all isotropic shifts in these comparative pairs, as is evident by, e.g., the reversal of 4-Me and 6-Me positions in the members of each pair (Figures 3 and 4). Nonetheless, except for the 2-H resonances, broadened by proximity to the cluster core, a given substituent undergoes a larger shift in a selenide vs sulfide cluster. The resonances that are most sensitive to both Q = S/Se and ligand L' differences are 4-Me, 5-H, and 6-Me of the coordinating arms (Figure 1). The 2'-H and 3'-H resonances of the legs exhibit smaller isotropic shifts and respond less sensitively and regularly to these changes. Consequently, they, and the nearly constant 4'-Me chemical shift, are not very useful in monitoring ligand substitution at the unique site, and are not further considered.

¹H Isotropic Shifts. The magnetic properties of [Fe₄Q₄]²⁺ clusters arise from exchange coupling.³³ Two Fe³⁺Fe²⁺ pairs are each coupled by double exchange; the resultant spins are in turn antiferromagnetically coupled to afford a diamagnetic ground state and paramagnetic excited states, the occupation of one or more of which produces the observed cluster paramagnetism. Isotropic shifts are defined in Table 2. The isotropic component of the proton chemical shifts of the

(29) Live, D. H.; Chan, S. I. *Anal. Chem.* **1970**, *42*, 791.

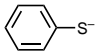
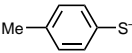
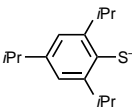
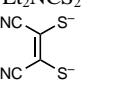
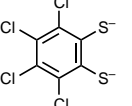
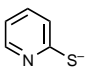
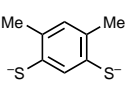
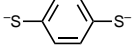
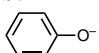
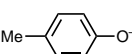
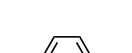
(30) Liu, H. Y.; Scharbert, B.; Holm, R. H. *J. Am. Chem. Soc.* **1991**, *113*, 9529.

(31) Spectra of protein-bound [Fe₄Q₄]²⁺ and [Fe₂Q₂]²⁺ clusters (Q = S, Se) have been presented, with chemical shifts of cysteinyl protons larger in the Q = Se cases.

(32) (a) Gaillard, J.; Moulis, J. M.; Meyer, J. *Inorg. Chem.* **1987**, *26*, 320. (b) Benini, S.; Ciurli, S.; Luchinat, C. *Inorg. Chem.* **1995**, *34*, 417.

(33) (a) Noodleman, L. *Inorg. Chem.* **1991**, *30*, 246, 256. (b) Bominaar, E. L.; Borshch, S. A.; Girerd, J.-J. *J. Am. Chem. Soc.* **1994**, *116*, 5362.

Table 2. ¹H NMR Isotropic Shifts and Redox Potentials of [Fe₄Q₄(LS₃)L']²⁻³⁻ Clusters (Q = S, Se) with Anionic L' Ligands in Acetonitrile Solutions at 297 K

no.	L'	$(\Delta H/H_0)_{\text{iso}}^a$ ppm				L' ^b	$E_{1/2}, \text{V}^c$
		2-H	4-Me	5-H	6-Me		
2 ^S	Cl ⁻	1.68	-1.67	-1.51	-1.59		-0.99
2 ^{Se}		1.15	-2.16	-1.79	-1.68		-0.97
3 ^S	CN ⁻	1.36	-1.71	-1.40	-1.51		-0.92, -1.73
3 ^{Se}		0.88	-2.12	-1.65	-1.58		-0.90, -1.55
4 ^S	MeS ⁻	1.52	-1.49	-1.43	-1.55	-13.3	<i>d</i>
4 ^{Se}		1.11	-1.99	-1.68	-1.64	-16.3	-1.08
5 ^S	EtS ⁻	1.57	-1.47	-1.42	-1.54	-10.7 (CH ₂), -1.13 (Me)	-1.11
5 ^{Se}		1.12	-1.98	-1.68	-1.64	-13.1 (CH ₂), -1.50 (Me)	-1.08
6 ^{Se}	<i>i</i> PrS ⁻	1.10	-1.97	-1.67	-1.64	-9.02 (CH); -1.81 (Me)	-1.11
7 ^{Se}	<i>t</i> BuS ⁻	1.08	-1.95	-1.67	-1.63	-1.91	-1.12
8 ^{Se}		1.05	-2.03	-1.70	-1.63	1.47, -1.08, 2.14	-1.01
9 ^S		1.53	-1.53	-1.43	-1.53	1.21, -0.83, -1.59	-1.05
9 ^{Se}		1.05	-2.02	-1.69	-1.63	1.41, -1.05, -1.88	-1.03
10 ^{Se}		1.03	-1.99	-1.67	-1.59	-0.41 (Me), -1.05, -0.02 (Me)	-1.08
11 ^{Se}	Et ₂ NCS ₂ ⁻	1.21	-1.99	-1.86	-1.75	-3.93 (CH ₂), -0.17 (Me)	-0.20, ^e -1.14 ^f
12 ^{Se}		1.62	-2.03	-2.01	-1.91		-0.35, ^e -1.22 ^f
13 ^{Se}		1.88	-2.03	-2.01	-2.00		-0.60, ^e -1.30 ^f
14 ^S		1.71	-1.52	-1.54	-1.64	<i>g</i>	<i>d</i>
14 ^{Se}		1.16	-2.06	-1.81	-1.73	<i>g</i>	-1.03
15 ^{Se}		1.05	-2.01	-1.68	-1.61	-2.67 (Me), -2.42 (5-H) ^h	-0.01, ^e -1.09 ^f
16 ^{Se}		1.08	-2.02	-1.69	-1.64	<i>i</i>	-1.06
17 ^S	S ²⁻	<i>h</i>	-1.88	-1.93	-2.25		-1.26, -1.53
17 ^{Se}	Se ²⁻	1.55	-2.27	-2.14	-2.33		-1.21, -1.46
18 ^{Se}		1.46	-2.15	-1.82	-1.74	2.01, -2.63, 2.98	-1.04
19 ^S		1.99	-1.62	-1.54	-1.66	-, -2.04, -2.39	<i>d</i>
19 ^{Se}		1.51	-2.14	-1.82	-1.74	2.20, -2.52, -2.88	-1.05
20 ^{Se}		1.45	-2.17	-1.83	-1.75	2.29, -2.38	-1.01
21 ^{Se}	MeCO ₂ ⁻	1.25	-2.17	-1.81	-1.70		-1.00

^a $(\Delta H/H_0)_{\text{iso}} = (\Delta H/H_0)_{\text{dia}} - (\Delta H/H_0)_{\text{obs}}$; diamagnetic reference shifts are those of (Bu₄N)₃LS₃, NaS₂CNEt₂, and free (protonated) ligands L' in acetonitrile. ^b For phenyl ligands, shifts are given in the order *ortho*, *meta*, *para*. ^c $E_{1/2} = (E_{\text{pc}} + E_{\text{pa}})/2$. ^d Not determined. ^e Oxidation. ^f Reduction. ^g Unassigned signals at 10.0, 11.0, 12.3 (Q = S) and 10.1, 11.0, 12.5 ppm (Q = Se). ^h 2-H signal not observed. ⁱ Not observed.

coordinated arms in [Fe₄S₄(LS₃)L']²⁻ clusters with [Fe₄S₄]²⁺ cores are concluded to be dominantly contact in origin because of the sign pattern of the isotropic shifts. Briefly, antiparallel ligand → metal spin delocalization leaves parallel spin on the odd-alternate benzenethiolate groups which is distributed via the π-system with positive spin density ρ^π_C at carbon atoms 2, 4, and 6 (Figure 1) and negative spin density at the other carbon atoms. From the definition of isotropic shifts, the relation for the electron-nuclear hyperfine coupling constant $A_i = Q_{\beta} \rho_{\text{C}}^{\pi}$ (Q_{CH} negative and Q_{CMe} positive), and standard contact shift theory,^{15,34} the pattern of observed shifts emerges. Resonances of 4-Me, 5-H, and 6-Me are displaced downfield while the 2-H signal is shifted upfield. Dominant contact shifts are a general property of [Fe₄S₄]²⁺ clusters.³⁵ These shifts are rather small, in the present case covering the range of ca. 1–2 ppm for the LS₃ ligand. Accurate values, therefore, depend on the most appropriate choice of diamagnetic reference. Here we have

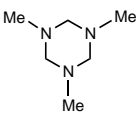
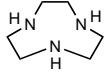
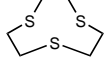
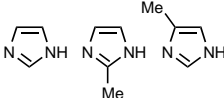
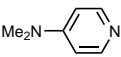
employed the references stated in Table 2 and utilize the isotropic shifts for internal comparison only rather than as absolute values. If the shifts are purely contact, they are proportional to the magnetic susceptibility χ^M. For a pair of selenide/sulfide clusters, the ratio of contact shifts of a given proton *i* at the same temperature is that of eq 3.

$$(\Delta H/H)_{\text{con}}^{\text{Se}} / (\Delta H/H)_{\text{con}}^{\text{S}} = A_i^{\text{Se}} \chi_{\text{Se}}^{\text{M}} / A_i^{\text{S}} \chi_{\text{S}}^{\text{M}} \quad (3)$$

Examination of the isotropic shift data in Tables 2–4 leads to four conclusions:

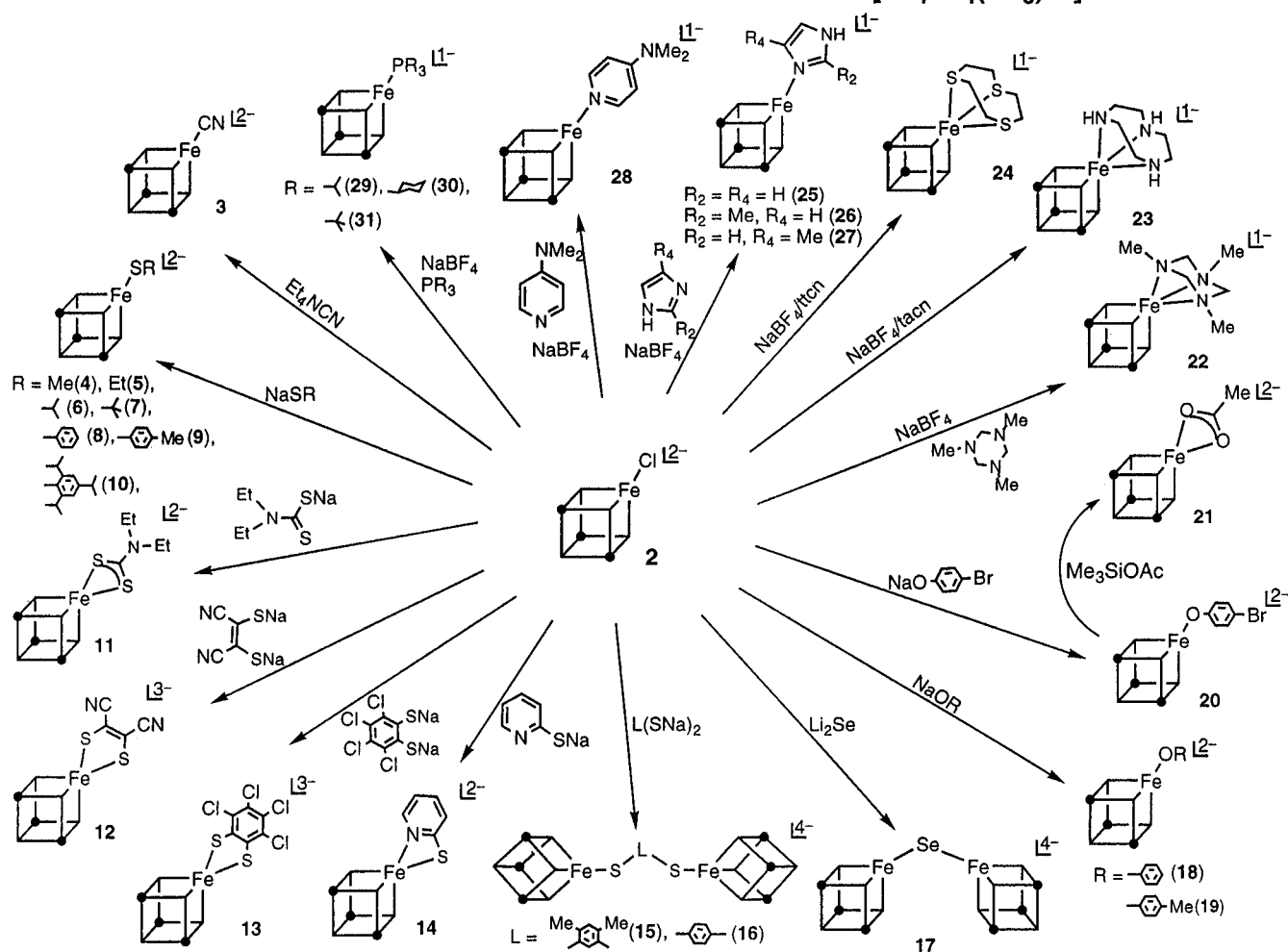
- (34) For a molecule with spin *S*, $(\Delta H/H)_{\text{con}}^i = -(A_i/\hbar)[g_{\text{av}}^2 \mu_{\text{B}}^2 S(S+1)/3\gamma_{\text{N}} kT]$. For application to [Fe₄S₄]²⁺ clusters, this expression must be modified to include population factors and summation over all populated levels.¹⁵
- (35) (a) Holm, R. H.; Phillips, W. D.; Averill, B. A.; Mayerle, J. J.; Herskovitz, T. *J. Am. Chem. Soc.* **1974**, *96*, 2109. (b) Reynolds, J. G.; Laskowski, E. J.; Holm, R. H. *J. Am. Chem. Soc.* **1978**, *100*, 5315.

Table 3. ^1H NMR Isotropic Shifts and Redox Potentials of $[\text{Fe}_4\text{Q}_4(\text{LS}_3)\text{L}]^-$ Clusters (Q = S, Se) with Neutral L' Ligands in Acetonitrile Solutions at 297 K^a

no.	L'	$(\Delta H/H_0)_{\text{iso}}$, ppm				$E_{1/2}$, V ^b
		2-H	4-Me	5-H	6-Me	
22 ^{Se}		1.54	-2.21	-1.97	-1.81	-0.94
23 ^S 23 ^{Se}		<i>d</i>	-1.73 -2.48	-1.82 -2.30	-1.98 -2.24	-1.18 -1.11
24 ^{Se}		1.34	-2.18	-2.05	-1.89	<i>e</i>
25 ^S , 26 ^S , 27 ^S 25 ^{Se} , 26 ^{Se} , 27 ^{Se}		1.64 1.07	-1.83 -2.27	-1.54 -1.80	-1.65 -1.69	-0.79, -0.78, -0.79 -0.78, -0.80, -0.79
28 ^S 28 ^{Se}		1.63 1.11	-1.83 -2.29	-1.53 -1.82	-1.64 -1.71	-0.82 -0.78
29 ^{Se} 30 ^{Se} 31 ^{Se}	<i>i</i> Pr ₃ P Cy ₃ P <i>t</i> Bu ₃ P	0.90 0.88 0.88	-2.22 -2.19 -2.22	-1.69 -1.69 -1.69	-1.69 -1.66 -1.69	-0.77 -0.81 -0.81

^a See footnotes *a* and *b* in Table 2. ^b $\Delta E_p = 75\text{--}120$ mV, with the large majority of values ≤ 100 mV. ^c Stoichiometric reactions: tacn CH_2 isotropic shifts are -6.67 and -13.1 ppm (Q = Se) and -5.83 and -9.70 ppm (Q = S). ^d Not observed. ^e Poorly defined redox step.

SITE-SPECIFIC SUBSTITUTION REACTIONS OF $[\text{Fe}_4\text{Se}_4(\text{LS}_3)\text{Cl}]^{2-}$

**Figure 2.** Summary of the ligand substitution reactions of $[\text{Fe}_4\text{Se}_4(\text{LS}_3)\text{Cl}]^{2-}$ (2) affording the cluster products 3–31. Monodentate and bidentate coordination cannot be distinguished in 21.

(i) Shifts of one or more of the substituents 4-Me, 5-H, and 6-Me on the LS_3 ligand arms are very sensitive to the nature of the ligand L' at the unique iron site (Tables 2 and 3). The signs

of all shifts are consistent with contact interactions, which are taken as dominant in all clusters.

(ii) Shifts of corresponding substituents on the LS_3 ligand

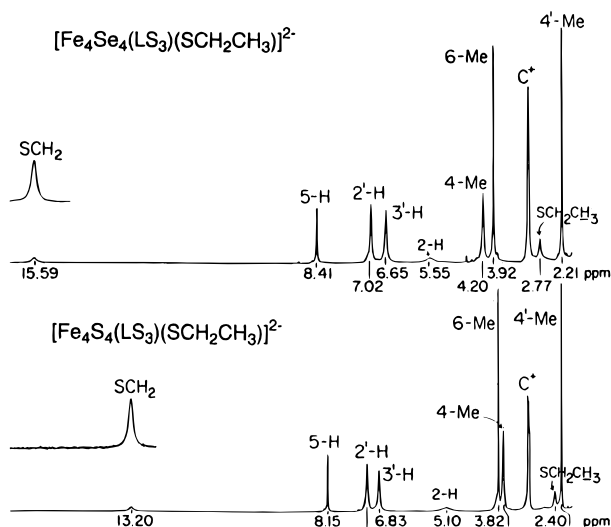


Figure 3. Comparative ¹H NMR spectra of [Fe₄Q₄(LS₃)(SEt)]²⁻ (Q = S, Se) in acetonitrile solution at 297 K. Signal assignments are indicated.

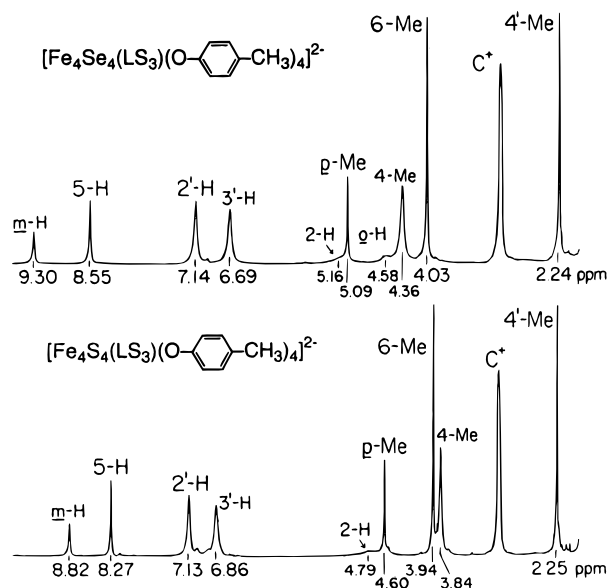


Figure 4. Comparative ¹H NMR spectra of [Fe₄Q₄(LS₃)(O-*p*-tol)]²⁻ (Q = S, Se) in acetonitrile solution at 297 K. Signal assignments are indicated.

arms and L' are always larger in selenide clusters than in sulfide clusters (with the exception of 2-H). These shifts are given as ratios in Table 4. The magnetic susceptibility ratios (299 K) for (Me₄N)₂[Fe₄Q₄(SPh)₄]¹⁷ and for (Me₄N)₃[Fe₄Q₄(SPh)₄]²⁰ are 1.30:1 and 1.17:1, respectively, in the solid state (299 K), indicating the selenide clusters to be less strongly coupled. For [Fe₄Q₄(LS₃)Cl]²⁻ in acetonitrile, the mean values of magnetic moments per cluster from three determinations of magnetic susceptibilities are $\mu_{\text{eff}} = 2.71 \mu_{\text{B}}$ (2^{Se}) and $2.58 \mu_{\text{B}}$ (2^S)³⁶ (294 K). These values correspond to the susceptibility ratio 1.10:1. The magnetic data are consistent with the larger isotropic shifts of selenide clusters in the cluster pairs of Table 3, provided that $A_i^{\text{Se}}/A_i^{\text{S}} \approx 1$.

(iii) The proposition that $A_i^{\text{Se}}/A_i^{\text{S}} \approx 1$ is supported by the essentially constant shift ratios for three [Fe₄Q₄(SR)₄]²⁻ cluster pairs (Table 4). In these clusters, the ligands can freely rotate

Table 4. Comparative Isotropic Shifts of [Fe₄Q₄]²⁺ Clusters (Q = S, Se) in Acetonitrile Solutions at 298 K

cluster	($\Delta H/H_0$) ^{Se} / $(\Delta H/H_0)$ ^S
[Fe ₄ Q ₄ (SEt) ₄] ²⁻	1.19 (CH ₂), 1.25 (Me)
[Fe ₄ Q ₄ (SPh) ₄] ²⁻ ^a	1.26 (<i>o</i> -H), 1.20 (<i>m</i> -H), 1.21 (<i>p</i> -H)
[Fe ₄ Q ₄ (S- <i>p</i> -C ₆ H ₄ Me) ₄] ²⁻	1.25 (<i>o</i> -H), 1.17 (<i>m</i> -H), 1.22 (<i>p</i> -H)
[Fe ₄ Q ₄ (LS ₃)Cl] ²⁻ ^b (2)	0.68 (2-H), 1.29 (4-Me), 1.19 (5-H), 1.06 (6-Me)
[Fe ₄ Q ₄ (LS ₃)(SEt)] ²⁻ (5)	0.71 (2-H), 1.35 (4-Me), 1.19 (5-H), 1.06 (6-Me), 1.22 (CH ₂), 1.30 (Me)
[Fe ₄ Q ₄ (LS ₃)(S- <i>p</i> -C ₆ H ₄ Me)] ²⁻ (9)	0.69 (2-H), 1.32 (4-Me), 1.18 (5-H), 1.07 (6-Me), 1.17 (<i>o</i> -H), 1.27 (<i>m</i> -H), 1.18 (<i>p</i> -H)
[Fe ₄ Q ₄ (LS ₃)(O- <i>p</i> -C ₆ H ₄ Me)] ²⁻ (19)	0.76 (2-H), 1.32 (4-Me), 1.18 (5-H), 1.05 (6-Me), 1.23 (<i>m</i> -H), 1.30 (<i>p</i> -H) ^c
[Fe ₄ Q ₄ (LS ₃)L'] ²⁻ (mean values of 11 pairs) ^e	0.69(4) ^d (2-H), 1.30(7) (4-Me), 1.18(4) (5-H), 1.06(3) (6-Me)

^a (Me₄N)₂[Fe₄Q₄(SPh)₄] (solid, 299 K): $\mu_{\text{eff}} = 2.47 \mu_{\text{B}}$ (Q = Se), 2.17 μ_{B} (Q = S).¹⁷ ^b Acetonitrile solution, 294 K: $\mu_{\text{eff}} = 2.71 \mu_{\text{B}}$ (Q = Se), 2.58 μ_{B} (Q = S). ^c *o*-H signal (Q = S) not resolved. ^d Esd of mean value. ^e 2-5, 9, 14, 17, 19, 23, 25, 28.

about C-S bonds and can assume random orientations with respect to the core atoms. For clusters 5, 9, and 19, the isotropic shift ratios of the ligands L' are also practically constant. However, this is not the case for the LS₃ shifts of 2 and all other Q = S/Se cluster pairs containing the LS₃ ligand. When 11 such pairs, each with constant L', are examined, there is a definite trend in the shift ratios at the 4-Me, 5-H, and 6-Me positions. The set includes species with four-, five- (14), and six-coordination (23) at the unique iron site (Table 4). Further, the shifts of 2-H in selenide clusters are *ca.* 30% less than those in sulfide clusters, the only instance of an isotropic shift reversal in all of the cluster pairs investigated. While we cannot give a precise reason for the small but real differences in electron delocalization in the selenide and sulfide clusters, it must be largely associated with the semirigid nature of the LS₃ ligand and changes in conformation produced by the different [Fe₄Q₄]²⁺ cores. Earlier, we estimated that the selenide core effective volume is 25% larger than the sulfide core volume and provided a rigorous conformational analysis of [Fe₄Q₄(LS₃)L']²⁻ clusters in terms of the tilt and cant angles of ligand arms and legs.^{8b} At least in their crystalline Ph₄P⁺ salts, the conformations of [Fe₄Q₄(LS₃)Cl]²⁻ are clearly different; even crystallographically inequivalent [Fe₄Se₄(LS₃)Cl]²⁻ clusters in the same asymmetric unit can differ somewhat in conformation.^{8b} Of the protons on the ligand arms, 2-H is most affected by conformation changes that alter its position in the shielding cone of the central benzene ring.^{8b} This proton is also nearest the core and may be influenced by weak but direct spin transfer from the core in addition to delocalization through the Fe-S-phenyl pathway. While we could not have predicted that 2-H isotropic shifts would be smaller in selenide than sulfide clusters, it is clearly the proton most likely to be influenced by variable ligand conformation.³⁷

(iv) The relative extent of spin delocalization in selenide vs sulfide clusters is nearly independent of L', as shown by the small variation in the ratio of shift ratios for given LS₃ and (to a lesser extent) L' substituents. This is illustrated for three [Fe₄Q₄(SR)₄]²⁻ and four [Fe₄Q₄(LS₃)L']²⁻ cluster pairs (Table 4); for example, among the latter the 4-Me ratio is 1:1.05:1.02:1.02 (in order of listing). The 5-H and 6-Me shift ratios are also essentially unity.

Substituted Clusters. The reactions of the clusters 2 are conveniently discussed in terms of anionic and neutral ligand

(36) This value is somewhat larger than the $\mu_{\text{eff}} = 2.1-2.3 \mu_{\text{B}}$ usually found for [Fe₄S₄L₄]²⁻ clusters at room temperature: (a) Wong, G. B.; Bobrik, M. A.; Holm, R. H. *Inorg. Chem.* **1978**, *17*, 578. (b) Laskowski, E. J.; Frankel, R. B.; Gillum, W. O.; Papaefthymiou, G. C.; Renaud, J.; Ibers, J. A.; Holm, R. H. *J. Am. Chem. Soc.* **1978**, *100*, 5322.

(37) These points are made by assuming contact shifts only, consistent with available evidence. We have no way of estimating any dipolar contributions to isotropic shifts arising from the zero-field splittings of integer-spin excited state(s) that may be populated.

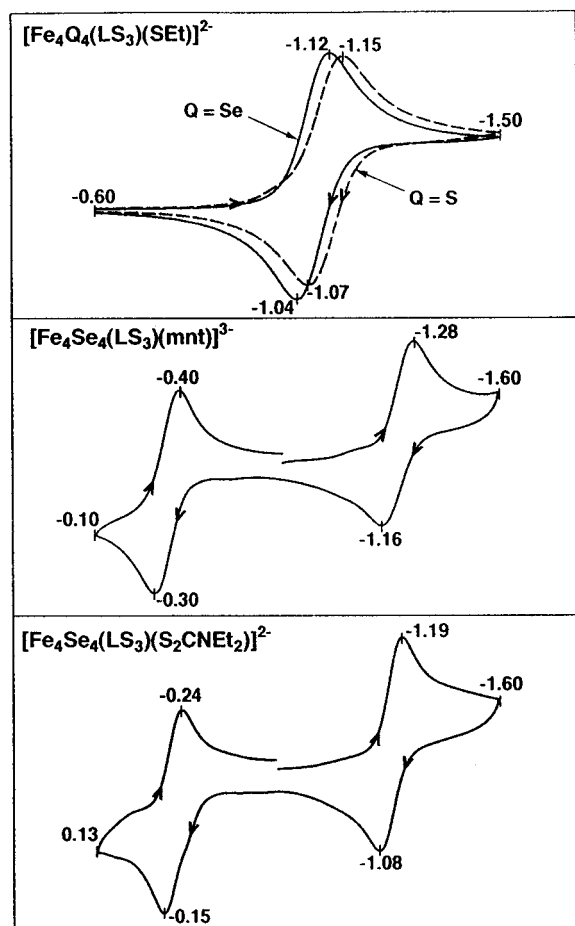


Figure 5. Cyclic voltammograms in acetonitrile solutions (20 mV/s, 297 K): (Top) $[\text{Fe}_4\text{Q}_4(\text{LS}_3)(\text{SET})]^{2-}$ ($\text{Q} = \text{S}, \text{Se}$); (middle) $[\text{Fe}_4\text{Se}_4(\text{LS}_3)(\text{mnt})]^{3-}$; (bottom) $[\text{Fe}_4\text{Se}_4(\text{LS}_3)(\text{S}_2\text{CNET}_2)]^{2-}$. Peak potentials are indicated.

substitution, with emphasis on the reactions of 2^{Se} . Reactions were readily monitored because of the resolved chemical shifts of initial and product clusters.

(a) Anionic Ligands. Clusters **3–21** formed by mono- and dinegative ligands are contained in Table 2. The reactions 1 and 2 in acetonitrile leading to these species, involving the ligands cyanide, thiolate, phenolate, dithiolate, dithiocarbamate, and selenide, are stoichiometric with little or no byproducts detected by NMR. Although we have not pursued the matter of relative potentials with a large number of $[\text{Fe}_4\text{Q}_4(\text{LS}_3)\text{L}]^{2-}$ cluster pairs, the available data reveal a small but consistent positive shift of redox potentials for the selenide clusters. This is illustrated by the voltammograms of the clusters **5** in Figure 5 (top). As is typical of $[\text{Fe}_4\text{Q}_4(\text{SR})_4]^{2-}$ species, both exhibit reversible 2-/3- redox steps, with the potential of 5^{Se} 30 mV more positive than that of 5^{S} . We have encountered no reversal of the trend $E_{\text{Se}} \leq E_{\text{S}}$ for $[\text{Fe}_4\text{S}_4]^{2+,+}$ couples in previous work^{17,18} and among over more than 10 comparative pairs in Tables 2 and 3. The trend is further upheld by the potentials ($E_{1/2}^{\text{S}}, E_{1/2}^{\text{Se}}$) in acetonitrile for the following more conventional cluster pairs: $[\text{Fe}_4\text{Q}_4\text{Cl}_4]^{2-}$ (−0.79, −0.75 V), $[\text{Fe}_4\text{Q}_4(\text{SET})_4]^{2-}$ (−1.32, −1.26 V).

With regard to other aspects of redox behavior, there are several instructive observations in Table 2. Given 5^{Se} as a reference cluster with all-thiolate ligation, replacement of ethanethiolate with dithiocarbamate in **11**^{Se} affords two reversible steps (Figure 5, lower), an oxidation ($[\text{Fe}_4\text{Se}_4]^{3+,2+}$) at −0.20 V and a reduction ($[\text{Fe}_4\text{Se}_4]^{2+,+}$) at −1.14 V. Because the latter potential is only 60 mV different from 5^{Se} (−1.08 V), we conclude that bidentate coordination by dithiocarbamate does

not strongly increase the electron density in the $[\text{Fe}_4\text{Se}_4]^{2+}$ state but, by means of its charge-separated resonance form, is effective as a source of electron density in stabilizing the oxidized ($[\text{Fe}_4\text{Se}_4]^{3+}$) state. The latter is usually unstable in $[\text{Fe}_4\text{Q}_4(\text{SR})_4]^{-}$ clusters, only one example (with very bulky ligands) having ever been isolated.³⁸ When a dithiolate ligand is coordinated at the unique iron site as in **12**^{Se} and **13**^{Se}, the cluster negative charge is increased by one unit and additional electron density is introduced into the core relative to 5^{Se} or the benzenethiolate cluster **8**^{Se} as references. This has the consequence of facilitating oxidation and thus shifting potentials to more negative values. The result is that both reversible oxidation and reduction steps can be observed, as seen in the voltammogram of **12**^{Se} (Figure 5, middle). Both of these effects represent ways of modulating redox potentials of protein-bound Fe_4Q_4 clusters, by an increase of coordination number with anionic sulfur ligands. On the other hand, cluster **14**^{Se} shows a reversible reduction (−1.03 V) but not a well-defined oxidation. Evidently, the pyridine donor functionality is not consequential relative to coordination of the thiolate sulfur atom. It is now our experience that bidentate coordination by anionic sulfur ligands³⁹ at a single site in Fe_4Q_4 clusters tends to stabilize the $[\text{Fe}_4\text{Q}_4]^{2+,3+}$ oxidation levels in acetonitrile, DMF, and Me_2SO solutions.¹⁰ In clusters with monodentate coordination at that site, the $[\text{Fe}_4\text{Q}_4]^{3+}$ level is generally obtainable only in solvents of very low nucleophilicity, such as dichloromethane.^{10,11}

When two $[\text{Fe}_4\text{Q}_4]^{2+}$ clusters are connected by sulfide or selenide, the cluster reduction steps are not independent. This has been previously observed for **17**^S in Me_2SO , where the potential difference is 220 mV.⁹ The same property applies to **17**^S and the new cluster **17**^{Se} in acetonitrile where the differences are 270 and 250 mV, respectively.⁴⁰ Attempts to prepare double cubanes with different bridge and core chalcogenide atoms by variation of the reaction giving **17**^{Se} (Figure 2) afforded species with multiple NMR signals indicative of mixed sulfide/selenide cores. Clusters of this sort have been prepared earlier by intercluster chalcogenide exchange.²¹ Separate reduction steps were not resolved by cyclic or differential pulse voltammetry for bridged clusters **15**^{Se} and **16**^{Se}, for which we estimate the nearest $\text{Fe}\cdots\text{Fe}$ intercluster separations to be $>7.8 \text{ \AA}$ in the expected transoid conformations.⁹ In **17**^{Se}, this distance is 3.94 \AA .⁴⁰

Last, we consider the redox behavior of cyanide-ligated clusters **3**, whose voltammograms are presented in Figure 6. Both clusters show two reversible reductions corresponding to the couples $[\text{Fe}_4\text{Q}_4]^{2+,+}$ and $[\text{Fe}_4\text{Q}_4]^{+,0}$. While the second reduction has been observed occasionally for $[\text{Fe}_4\text{S}_4\text{L}_4]^{2-}$ species,⁴¹ it is absent or chemically irreversible in the vast majority of clusters with $\text{L} = \text{RS}^-, \text{RO}^-$, or halide examined in acetonitrile, DMF, and Me_2SO . Presumably the encapsulating nature of the LS_3 ligand, with a small contribution from the π -acid property of cyanide, helps stabilize the all-ferrous cores

(38) O'Sullivan, T.; Millar, M. M. *J. Am. Chem. Soc.* **1985**, *107*, 4096.

(39) For earlier examples with dithiocarbamate-bound Fe_4S_4 clusters, cf.: Kanatzidis, M. G.; Coucouvanis, D.; Simopoulos, A.; Kostikas, A.; Papaefthymiou, V. *J. Am. Chem. Soc.* **1985**, *107*, 4925.

(40) The bridged structure has been demonstrated by the X-ray structure determination of $(\text{Bu}_4\text{N})_4[\text{17}^{\text{Se}}]$, in which the $\text{Fe}-\text{Se}-\text{Fe}$ bridge angle is 113 and 115° (two independent anions). This information is included in a forthcoming report of the synthesis and properties of sulfide- and selenide-bridged double cubane clusters: Huang, J.; Mukerjee, S.; Segal, B. M.; Akashi, H.; Zhou, J.; Holm, R. H. Submitted for publication.

(41) (a) For example, the $[\text{Fe}_4\text{S}_4(\text{SPh})_4]^{3-,4-}$ couple has been observed at -1.72 V in acetonitrile: Cambray, J.; Lane, R. W.; Wedd, A. G.; Johnson, R. W.; Holm, R. H. *Inorg. Chem.* **1977**, *16*, 2565. (b) See also: Pickett, C. J. *J. Chem. Soc., Chem. Commun.* **1985**, 323.

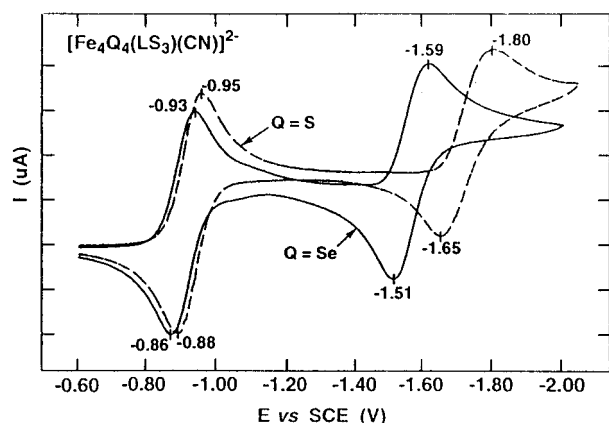
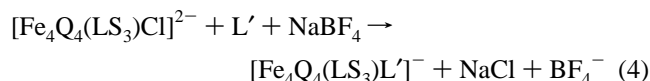


Figure 6. Cyclic voltammograms in acetonitrile solutions (20 mV/s, 297 K) of $[\text{Fe}_4\text{Q}_4(\text{LS}_3)(\text{CN})]^{2-}$ ($\text{Q} = \text{S}, \text{Se}$). Peak potentials are indicated.

$[\text{Fe}_4\text{Q}_4]^0$, one of which has recently been isolated in the form of $[\text{Fe}_4\text{S}_4(\text{PR}_3)_4]$.⁴² Even more surprising is the 180-mV difference in potential for the second reduction. This is the largest difference known for any pair of isoelectronic $[\text{Fe}_4\text{Q}_4]^{z,z-1}$ couples and may be compared to typical values of <50 mV for the $[\text{Fe}_4\text{Q}_4]^{2+,+}$ couples. Evidently, the difference in chalcogenide character of the redox-active orbitals in the $[\text{Fe}_4\text{Q}_4]^{+,0}$ step is larger than in preceding redox steps.

(b) Neutral Ligands. Clusters **22–31** containing neutral ligands L' are collected in Table 3 together with their isotropic shifts and redox potentials. They were generated by reaction 4



in acetonitrile, in which excess NaBF_4 (4 equiv) in methanol removes chloride from **2** in the presence of ≥ 3 equiv of L' . In the cases tested, there was no reaction of the cluster with at least 3 equiv of ligand in the absence of NaBF_4 . The ligand set includes cyclic triamines, a cyclic trisulfide, imidazoles, a substituted pyridine, and tertiary phosphines. Although multiple attempts were made, only the cluster **24^{Se}** could be obtained in crystalline form suitable for an X-ray study.

Cluster **24^{Se}** was crystallized in the form $(\text{Bu}_4\text{N})[\text{Fe}_4\text{Se}_4(\text{LS}_3)(\text{[9]aneS}_3)] \cdot \text{[9]aneS}_3$. Its structure is only the fourth that has been determined for an LS_3 -bound cluster,^{8,13} whose salts usually form only microcrystalline solids. The structure of the $[\text{9]aneS}_3$ solvate molecule is similar to that reported⁴³ and is not considered further. The structure of the entire cluster anion, shown in Figure 7, reveals the *ababab* conformation,⁸ in which phenylthio substituents alternate in position above and below the central benzene ring. Atom $\text{Se}(3)$ is positioned 3.73 \AA above the central benzene ring, indicating that the $[\text{Fe}_4\text{Se}_4]^{2+}$ core is substantially immersed in the ligand cavity defined by atoms $\text{S}(11\text{--}13)$ and the inward edges of the three phenylthio arms. The corresponding distances are $3.68, 3.69,$ and 4.09 \AA in three crystallographically independent clusters **2^{Se}**, for which a detailed conformational analysis has been presented.^{8b} No symmetry is imposed on the anion. The cluster core with its

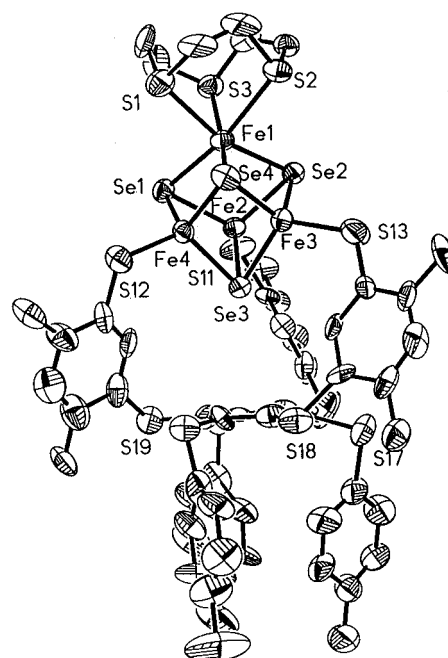


Figure 7. Overall structure of $[\text{Fe}_4\text{Se}_4(\text{LS}_3)(\text{[9]aneS}_3)]^{-}$, showing the *ababab* ligand conformation, the atom-labeling scheme, and 50% probability ellipsoids.

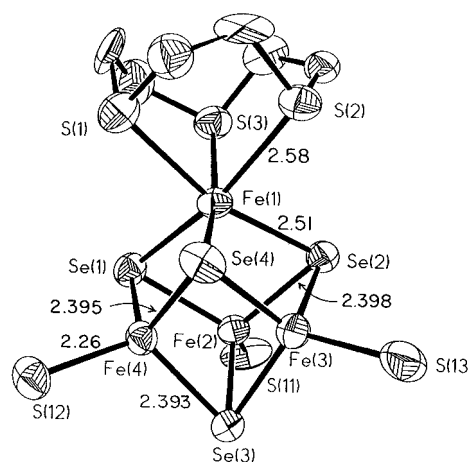


Figure 8. Structure of the cluster portion of $[\text{Fe}_4\text{Se}_4(\text{LS}_3)(\text{[9]aneS}_3)]^{-}$, with the atom-labeling scheme, 50% probability ellipsoids, and bond distances (\AA) averaged under trigonal symmetry.

terminal ligands is shown in Figure 8. Cluster dimensions are comparable to those for other $[\text{Fe}_4\text{Se}_4\text{L}_4]^{2-}$ clusters ($\text{L} = \text{Cl}^{-}, \text{Br}^{-}, \text{PhS}^{-}$).⁴⁴ However, the core does not show the compressed tetragonal D_{2d} structure common to $[\text{Fe}_4\text{Q}_4]^{2+}$ clusters but rather a trigonal distortion engendered by coordination of $[\text{9]aneS}_3$ and LS_3 . Metric data in Table 5 are arranged such that idealized trigonal symmetry is evident. Thus, the three $\text{Fe}(1)\text{--Se}$ distances are considerably longer (mean $2.51(2) \text{ \AA}$) than all other $\text{Fe}\text{--Se}$ distances (mean $2.396(7) \text{ \AA}$). The same is true of the three $\text{Fe}(1)\text{--Fe}$ distances (mean $2.95(1) \text{ \AA}$) compared to the other three $\text{Fe}\text{--Fe}$ separations (mean $2.810(9) \text{ \AA}$). Note also that the six $\text{Fe}\text{--Se}\text{--Fe}$ angles in the rhombic faces of the core containing $\text{Fe}(1)$ are distinguishable from other such angles involving $\text{Fe}(2\text{--}4)$, consistent with trigonal symmetry.

Cluster **24^{Se}** is the first structurally characterized $[1:3]$ site-differentiated Fe_4Q_4 cluster with a six-coordinate iron atom. The

(42) Goh, C.; Segal, B. M.; Huang, J.; Long, J. R.; Holm, R. H. *J. Am. Chem. Soc.* **1996**, *118*, 11844. No X-ray structure of this cluster oxidation state is available; however, stoichiometry implies tetrahedral coordination and therewith an electronic structure unlike that of $[\text{Fe}_4\text{S}_4(\text{CO})_{12}]$, which contains six-coordinate $\text{Fe}(\text{II})$ and whose structural parameters indicate a diamagnetic compound: Nelson, L. L.; Lo, F. Y.-K.; Rae, A. D.; Dahl, L. F. *J. Organomet. Chem.* **1982**, *225*, 309.

(43) (a) Glass, R. S.; Wilson, G. S.; Setzer, W. N. *J. Am. Chem. Soc.* **1980**, *102*, 5068. (b) Cristiani, F.; Devillanova, F. A.; Isaia, F.; Lippolis, V.; Verani, G.; Demartin, F. *Heteroatom Chem.* **1993**, *4*, 571.

(44) (a) Cen, W.; Liu, H. *Jiegou Huaxue (J. Struct. Chem.)* **1986**, *5*, 203. (b) Fenske, D.; Maué, P.; Merzweiler, K. *Z. Naturforsch.* **1987**, *B42*, 928. (c) Rutchik, S.; Kim, S.; Walters, M. A. *Inorg. Chem.* **1988**, *27*, 1513. (d) Ahle, A.; Dehnicke, K.; Maichle-Mosmer, J.; Strähle, J. Z. *Naturforsch.* **1994**, *B49*, 434.

Table 5. Selected Interatomic Distances (Å) and Angles (deg) for $[\text{Fe}_4\text{Se}_4(\text{LS}_3)(\text{[9]aneS}_3)]^+$

Terminal Ligands			
Fe(2)–S(11)	2.263(6)	S(1)–Fe(1)–S(2)	80.7(2)
Fe(3)–S(13)	2.244(7)	S(1)–Fe(1)–S(3)	80.5(2)
Fe(4)–S(12)	2.272(6)	S(2)–Fe(1)–S(3)	80.7(2)
mean of 3	2.26(1)	S(1)–Fe(1)–Se(1)	93.4(2)
Fe(1)–S(1)	2.578(7)	S(1)–Fe(1)–Se(4)	84.8(2)
Fe(1)–S(2)	2.602(3)	S(3)–Fe(1)–Se(1)	85.3(2)
Fe(1)–S(3)	2.564(6)	S(2)–Fe(1)–Se(2)	83.8(2)
mean of 3	2.58(2)	S(2)–Fe(1)–Se(4)	91.0(2)
		S(3)–Fe(1)–Se(2)	92.2(2)
Core			
Fe(1)–Se(1)	2.523(4)	Fe(1)–Fe(2)	2.959(3)
Fe(1)–Se(2)	2.485(3)	Fe(1)–Fe(3)	2.962(4)
Fe(1)–Se(4)	2.513(3)	Fe(1)–Fe(4)	2.938(4)
mean of 3	2.51(2)	mean of 3	2.95(1)
		Fe(2)–Fe(3)	2.803(4)
Fe(2)–Se(2)	2.398(4)	Fe(3)–Fe(4)	2.820(4)
Fe(3)–Se(4)	2.400(4)	Fe(2)–Fe(4)	2.806(4)
Fe(4)–Se(1)	2.401(3)	mean of 3	2.810(9)
Fe(2)–Se(1)	2.393(3)		
Fe(3)–Se(2)	2.387(3)	Fe(2)–Fe(1)–Fe(3)	56.51(9)
Fe(4)–Se(4)	2.406(4)	Fe(4)–Fe(1)–Fe(3)	57.1(1)
Fe(2)–Se(3)	2.386(3)	Fe(4)–Fe(1)–Fe(2)	56.83(9)
Fe(3)–Se(3)	2.399(4)	mean of 3	56.8(3)
Fe(4)–Se(3)	2.395(3)		
mean of 9	2.396(7)	Fe(4)–Fe(3)–Fe(1)	61.0(1)
		Fe(2)–Fe(3)–Fe(1)	61.68(9)
		Fe(4)–Fe(2)–Fe(1)	61.21(9)
		mean of 3	61.3(3)
Fe(3)–Fe(2)–Fe(4)	60.4(1)	Fe(2)–Fe(4)–Fe(1)	61.96(9)
Fe(2)–Fe(4)–Fe(3)	59.8(1)	Fe(3)–Fe(4)–Fe(1)	61.9(1)
Fe(2)–Fe(3)–Fe(4)	59.9(1)	Fe(3)–Fe(2)–Fe(1)	61.8(1)
mean of 3	60.0(3)	mean of 3	61.9(1)
Se(1)–Fe(1)–Se(4)	101.7(1)	Se(1)–Fe(2)–Se(3)	105.3(1)
Se(2)–Fe(1)–Se(4)	100.4(1)	Se(2)–Fe(3)–Se(3)	105.7(1)
Se(2)–Fe(1)–Se(1)	100.5(1)	Se(1)–Fe(4)–Se(3)	104.8(1)
Se(1)–Fe(2)–Se(2)	107.0(1)	Se(4)–Fe(3)–Se(3)	105.0(1)
Se(2)–Fe(3)–Se(4)	106.7(1)	Se(2)–Fe(2)–Se(3)	105.8(1)
Se(1)–Fe(4)–Se(4)	108.7(1)	Se(4)–Fe(4)–Se(3)	104.9(1)
Fe(1)–Se(1)–Fe(4)	73.2(1)	Fe(1)–Se(1)–Fe(2)	74.0(1)
Fe(1)–Se(2)–Fe(2)	74.6(1)	Fe(1)–Se(2)–Fe(3)	74.8(1)
Fe(1)–Se(4)–Fe(3)	74.1(1)	Fe(1)–Se(4)–Fe(4)	73.3(1)
Fe(2)–Se(1)–Fe(4)	71.7(1)	Fe(2)–Se(3)–Fe(3)	71.7(1)
Fe(3)–Se(4)–Fe(4)	71.9(1)	Fe(2)–Se(3)–Fe(4)	71.9(1)
Fe(3)–Se(2)–Fe(2)	71.7(1)	Fe(3)–Se(3)–Fe(4)	72.1(1)

mean Fe–S(1–3) bond distance of 2.58(2) Å to [9]aneS₃ is incompatible with localized low-spin Fe(II,III) formulations such as apply to the complexes $[\text{Fe}(\text{[9]aneS}_3)_2]^{2+}$,^{45a} $\text{Fe}(\text{[9]aneS}_3)(\text{[9]aneS}_3\text{O})^{2+}$,^{45b} and $[\text{Fe}(\text{[9]aneS}_3)_2]^{3+}$.⁴⁶ Instead, the unique iron atom would appear to be biased toward the high-spin Fe(III) condition based on the mean Fe–S bond distance of 2.57(3) Å in high-spin $[\text{Fe}(\text{[9]aneS}_3)\text{Cl}_3]$.⁴⁷ The difference between mean values of the core Fe(1)–Se and Fe(2–4)–Se bond lengths (0.18 Å) is consistent with the difference between high-spin octahedral and tetrahedral Fe(III) radii (0.15 Å).⁴⁸ Whatever may be the exact charge distribution, the magnetic coupling within the $[\text{Fe}_4\text{Se}_4]^{2+}$ core is not strongly perturbed compared to other clusters. The isotropic shifts, although somewhat higher in this and other clusters (**22**^{Se}, **23**) having a six-coordinate site, still indicate a diamagnetic ground state.

(45) (a) Wieghardt, K.; Küppers, H.-J.; Weiss, J. *Inorg. Chem.* **1985**, *24*, 3067. (b) Küppers, H.-J.; Wieghardt, K.; Nuber, B.; Weiss, J.; Bill, E.; Trautwein, A. X. *Inorg. Chem.* **1987**, *26*, 3762.

(46) Blake, A. J.; Holder, A. J.; Hyde, T. I.; Schröder, M. *J. Chem. Soc., Chem. Commun.* **1989**, 1433.

(47) Ballester, J.; Parker, O. J.; Breneman, G. L. *Acta Crystallogr.* **1994**, *C50*, 712.

(48) Shannon, R. D. *Acta Crystallogr.* **1976**, *A32*, 751.

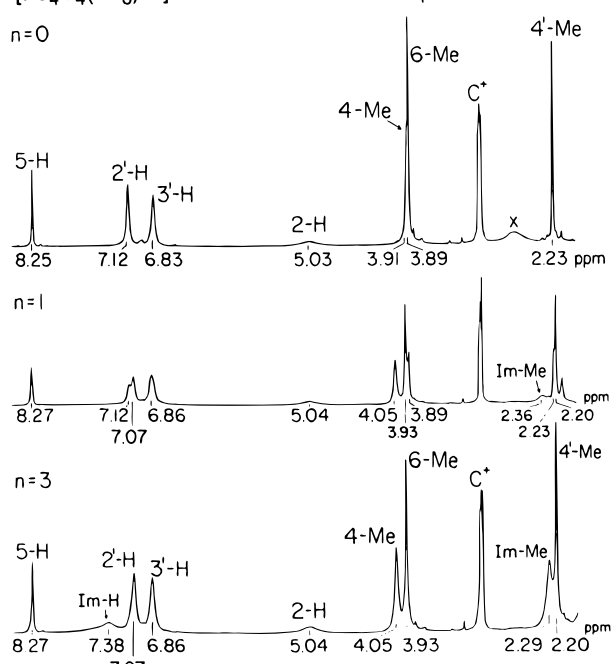
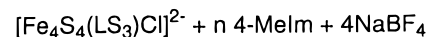


Figure 9. ¹H NMR spectra of the reaction systems of $[\text{Fe}_4\text{S}_4(\text{LS}_3)\text{Cl}]^{2-}$ with $n = 0$ –3 equiv of 4-methylimidazole in the presence of 4 equiv of NaBF_4 . Signal assignments are indicated.

Finally, the structure of **24**^{Se} proves at once that an iron site in an $[\text{Fe}_4\text{Q}_4]^{2+}$ cluster can sustain six-coordination with non-oxygen ligands. In enzyme-inhibitor complexes of aconitase, five- and six-coordinate unique sites of the $\text{FeS}_3\text{O}_{2,3}$ types have been detected crystallographically⁴⁹ in the $[\text{Fe}_4\text{S}_4]^{2+}$ cluster of the active form.

(c) Imidazole-Ligated Clusters. Among additional observations, it was found that the clusters **2** bind imidazoles to give **25**–**27** and the basic derivative 4-(dimethylamino)pyridine (but not pyridine itself) to afford **28**. Limiting isotropic shifts of **25**^S–**27**^S and of **25**^{Se}–**27**^{Se} are not distinguishable, and redox potentials within these sets are practically identical (Table 3). Also, **2**^{Se} binds the more basic tertiary phosphines, whose different substituents have almost no effect on isotropic shifts and redox potentials of clusters **29**^{Se}–**31**^{Se}. This is the first demonstration of the binding of unsaturated nitrogen ligands and phosphines to the $[\text{Fe}_4\text{Q}_4]^{2+}$ core. In the reaction systems $2/\geq 3\text{L}'/4\text{NaBF}_4$ represented by reaction 4, bound and free ligand L' are in fast exchange and **2** and $[\text{Fe}_4\text{Q}_4(\text{LS}_3)\text{L}']^{1-}$ are in slow exchange on the NMR time scale. Given the large cone angles of the phosphine ligands (160–182°) and structural characterization of $[\text{Fe}_4\text{S}_4(\text{PR}_3)_4]^+$ clusters with these phosphines, it is certain that only one such ligand binds.

Particular interest attends imidazole binding because the first example of a native imidazole-ligated cluster, $[\text{Fe}_4\text{S}_4(\text{Cys-S})_3(\text{His-N})]$, has been discovered by crystallography in *Desulfovibrio gigas* hydrogenase.⁵⁰ The course of imidazole binding in this work is typified by the system **2**^S/ n 4-MeIm/4NaBF₄ in Figure 9. With no added ligand, the spectrum is identical with that of **2**^S in the absence of NaBF₄. When $n =$

(49) (a) Lauble, H.; Kennedy, M. C.; Beinert, H.; Stout, C. D. *Biochemistry* **1992**, *31*, 2735; *J. Mol. Biol.* **1994**, *237*, 437. (b) Lauble, H.; Stout, C. D. *Proteins* **1995**, *22*, 1. (c) Lauble, H.; Kennedy, M. C.; Emptage, M. H.; Beinert, H.; Stout, C. D. *Proc. Natl. Acad. Sci. U.S.A.* **1996**, *93*, 13699.

(50) (a) Volbeda, A.; Charon, M.-H.; Piras, C.; Hatchikian, E. C.; Frey, M.; Fontecilla-Camps, J. C. *Nature* **1995**, *373*, 580. (b) Volbeda, A.; Garcin, E.; Piras, C.; de Lacey, A. L.; Fernandez, V. M.; Hatchikian, E. C.; Frey, M.; Fontecilla-Camps, J. C. *J. Am. Chem. Soc.* **1996**, *118*, 12989.

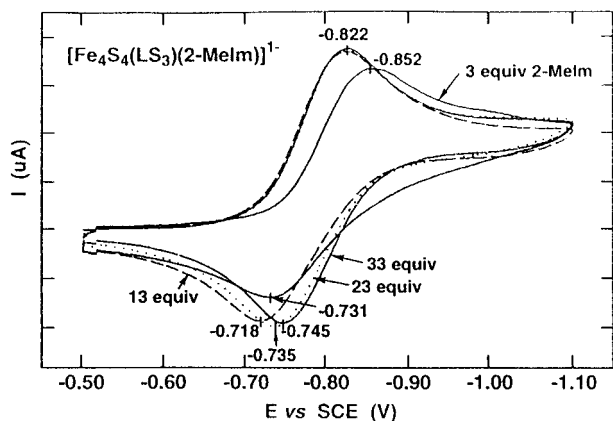


Figure 10. Cyclic voltammogram of $[\text{Fe}_4\text{S}_4(\text{LS}_3)(2\text{-Melm})]^{1-}$ (2 mM) in the presence of excess amounts of ligand in acetonitrile solution (20 mV/s, 297 K). Peak potentials are indicated.

1 equiv, new signals appear at 3.93 (4-Me), 4.05 (6-Me), and 7.07 (2'-H) ppm, and the 5-H resonance at 8.27 ppm is broadened and very slightly shifted. The new signals are assigned to imidazole-bound cluster 27^S . At $n = 3$ equiv, the new peaks intensify and the broadened signals of the exchanging ligand are evident. In this system, the reaction is complete at $n = 3$ equiv because the resonances of 2^S are no longer evident and the addition of a larger excess of ligand produces no change in the LS_3 signals of 27^S . The behavior is very similar in the other reaction systems producing clusters $25\text{--}28$. In all cases, only one new spectrum arises with added ligand, whose features are not broadened or shifted by variations in the initial $L':2^S$ mol ratio. Barring accidental degeneracy in *all* resolved LS_3 chemical shifts of clusters with one, and with more than one, bound ligand, we conclude that $25\text{--}28$ are properly formulated as monoligated by L' .

All potentials in Table 3 refer to the $[\text{Fe}_4\text{Q}_4]^{2+,+}$ couple. Although the clusters 23 are uninegative, their potentials of -1.18 V (23^S) and -1.11 V (23^{Se}) are comparable to (or more negative than) those of dinegative clusters (Table 2). This behavior obtains because electron donation to the core by the tridentate tacn ligand compensates the behavior of one monodentate anionic ligand. All other potentials of uninegative clusters are substantially less negative and occur in the interval -0.77 to -0.82 V. The voltammogram of 26^S , shown in Figure 10, is representative of the systems $2/nL'/4\text{NaBF}_4/0.1$ M (Bu₄N)-(PF₆) in acetonitrile. Addition of $n = 3$ equiv of 2-Melm shifts initial potential of -0.99 V (2^S) in the positive direction by 200 mV. Further increments of ligand cause peak potential shifts of *ca.* 30 mV until the limiting potential (-0.78 V) and peak separation (77 mV) are reached near 30 equiv of ligand. In general, $n > 3$ equiv of ligand decreased the peak separation and resulted in a closer approach to the criterion $i_{\text{pc}}/i_{\text{pa}} = 1$ for chemical reversibility. With ethanethiolate-ligated cluster 5^S as a reference, replacement of thiolate with 4-Melm (27^S) results in a positive potential shift of 320 mV. We take this value as the best available *estimate* of the intrinsic potential difference between $[\text{Fe}_4\text{S}_4(\text{Cys-S})_4]$ and $[\text{Fe}_4\text{S}_4(\text{Cys-S})_3(\text{His-N})]$ clusters.

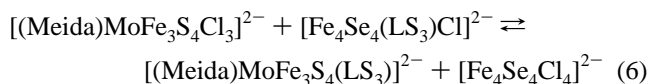
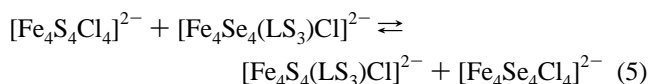
The electron transfer pathway in *D. gigas* hydrogenase consists of the alignment proximal- $\text{Fe}_4\text{S}_4|\text{Fe}_3\text{S}_4|\text{distal-Fe}_4\text{S}_4$ proceeding outward from the Ni-Fe active site.⁵⁰ The distal cluster is coordinated by the side chain of one histidyl residue, and the proximal cluster has the common $[\text{Fe}_4\text{S}_4(\text{Cys-S})_4]$ ligation. The redox potentials at pH 8 are -410 mV for the proximal cluster and -350 mV for the distal cluster.⁵¹ Judging from the method of determination, the difference in potentials

Table 6. Equilibrium Constants for Ligand Exchange between Clusters in Acetonitrile

system	reactants	K_{eq} (297 K)
A	$[\text{Fe}_4\text{S}_4\text{Cl}_4]^{2-} + [\text{Fe}_4\text{Se}_4(\text{LS}_3)\text{Cl}]^{2-}$	0.45
B	$[\text{Fe}_4\text{S}_4(\text{SEt})_4]^{2-} + [\text{Fe}_4\text{Se}_4(\text{LS}_3)(\text{SEt})]^{2-}$	0.50
C	$[(\text{Meida})\text{MoFe}_3\text{S}_4\text{Cl}_3]^{2-} + [\text{Fe}_4\text{S}_4(\text{LS}_3)\text{Cl}]^{2-}$	0.55
D	$[(\text{Meida})\text{MoFe}_3\text{S}_4\text{Cl}_3]^{2-} + [\text{Fe}_4\text{Se}_4(\text{LS}_3)\text{Cl}]^{2-}$	0.48
E	$[(\text{Cl}_4\text{cat})(\text{MeCN})\text{MoFe}_3\text{S}_4\text{Cl}_3]^{2-} + [\text{Fe}_4\text{S}_4(\text{LS}_3)\text{Cl}]^{2-}$	0.20
F	$[(\text{Cl}_4\text{cat})(\text{MeCN})\text{MoFe}_3\text{S}_4\text{Cl}_3]^{2-} + [\text{Fe}_4\text{Se}_4(\text{LS}_3)\text{Cl}]^{2-}$	0.16
G	$[\text{Fe}_4\text{S}_4(\text{LS}_3)(\text{SEt})]^{2-} + [\text{Fe}_4\text{Se}_4(\text{LS}_3)\text{Cl}]^{2-}$	1.5
H	$[\text{Fe}_4\text{S}_4(\text{LS}_3)(\text{CN})]^{2-} + [\text{Fe}_4\text{Se}_4(\text{LS}_3)\text{Cl}]^{2-}$	1.4
I	$[\text{Fe}_4\text{S}_4(\text{LS}_3)\text{Cl}]^{2-} + [\text{Fe}_4\text{Se}_4(\text{LS}_3)(\text{OC}_6\text{H}_4\text{-}p\text{-Br})]^{2-}$	0.97

is more significant than their absolute values. If the proximal cluster is taken as the reference, the sign of the ligand substitution effect is the same but the difference of 60 mV is much less than the estimated intrinsic value of 320 mV. Part of this difference may be attenuated by protein hydrogen-bonding and other environmental differences at the proximal and distal clusters. Such effects lead to a variation of over 300 mV for $[\text{Fe}_4\text{S}_4]^{2+,+}$ potentials of $[\text{Fe}_4\text{S}_4(\text{Cys-S})_4]$ clusters.⁵² Further, both hydrogenase potentials, as well as some in the foregoing range, are pH-dependent.

Ligand Exchange and Binding Affinities. Noting the conformational differences implied by the ¹H NMR results for the LS_3 ligand when bound to the two $[\text{Fe}_4\text{Q}_4]^{2+,+}$ cores, we sought to learn whether there is a detectable preference of the ligand for one core over the other. Consequently, reaction systems A–F in Table 6 were examined in acetonitrile solutions at ambient temperature. In no previous context had we entertained the possibility of exchange of tridentate LS_3 between clusters, as exemplified by reactions 5 and 6. In fact, these



and related reactions do occur and slowly reach equilibrium over a period of hours or several days; the equilibrium components are readily identified by their characteristic NMR spectra. No core chalcogenide exchange was observed; this process is extremely slow for $[\text{Fe}_4\text{Q}_4]^{2+,+}$ clusters at room temperature.²¹ While no kinetics data are available, exchange of unidentate ligands between $[\text{Fe}_4\text{S}_4(\text{SR})_4]^{2-}$ and $[\text{Fe}_4\text{Se}_4(\text{SR})_4]^{2-}$ to give an essentially statistical mixture of clusters occurs within several minutes or less after mixing.

Reaction systems A, E, and F are illustrated in Figure 11; the cubane-type MoFe_3S_4 clusters in systems C–F have been prepared previously.^{40,53} In system A (top spectrum), the partial conversion of 2^{Se} to 2^S is clear from the fully resolved spectra; $K_{\text{eq}} = 0.45$ and $\Delta G = 0.47$ kcal/mol. If, in the simplest analysis, $\Delta S = 0$, cluster solvation enthalpies cancel, and Fe–Cl and Fe–SEt bond energies are independent of Q, there is an apparent slight enthalpic preference for binding of LS_3 to the $[\text{Fe}_4\text{Se}_4]^{2+,+}$ core in systems A and B. In systems C–F, the bond energy equality is less certain inasmuch as the iron atoms do not necessarily have the same charge. These systems were investigated primarily to see if LS_3 transfer has generality. The occurrence of ligand transfer is particularly clear in these cases because LS_3 moves to a cluster with an $S = 3/2$ ground state and larger isotropic shifts. Thus, for systems E (middle

(51) Roberts, L. M.; Lindahl, P. A. *J. Am. Chem. Soc.* **1995**, *117*, 2565.

(52) Stephens, P. J.; Jollie, D. R.; Warshel, A. *Chem. Rev.* **1996**, *96*, 2491.

(53) Demadis, K. D.; Coucouvanis, D. *Inorg. Chem.* **1995**, *34*, 436.

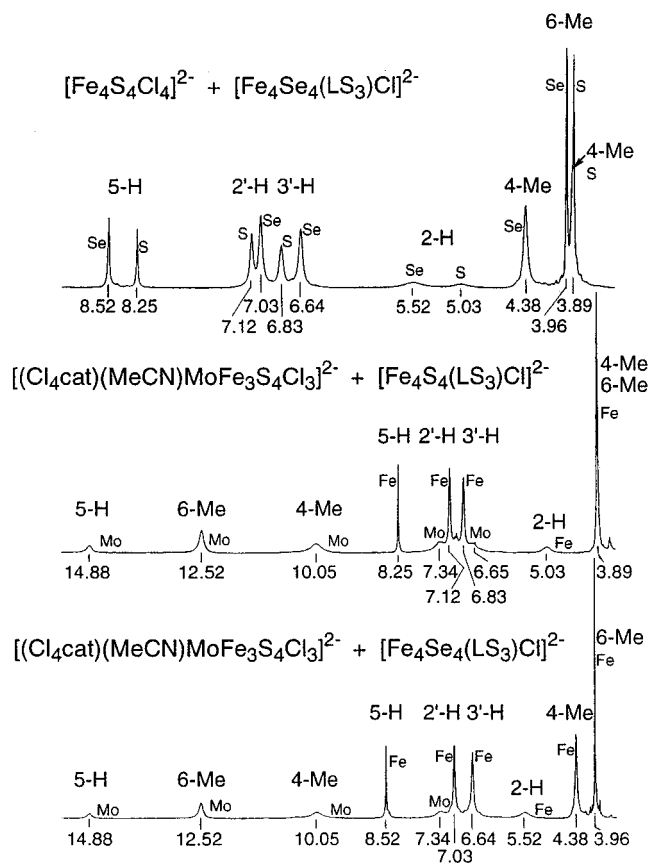
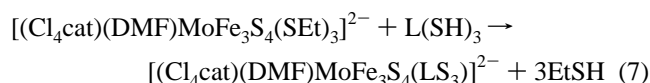


Figure 11. ^1H NMR spectra in acetonitrile solutions (297 K) demonstrating transfer reactions of the LS_3 ligand in the indicated cluster systems. Signals are designated as belonging to sulfide or selenide clusters (top) and MoFe_3S_4 (Mo) and Fe_4Q_4 (Fe) clusters (middle, bottom).

spectrum) and **F** (bottom spectrum), the appearance of 4-Me, 5-H, and 6-Me signals in the 10–15 ppm region is proof that ligand transfer has occurred. These features with only minor chemical shift differences have been found for the isolated product of reaction 7.⁵⁴ In systems **C–F**, there is an apparent



modest preference for the binding of LS_3 to the $[\text{Fe}_4\text{Q}_4]^{2+}$ core. However, the equilibrium constants do not differ largely from the statistical value of unity and the free energy changes are too small (–0.2 to 1.1 kcal/mol) to interpret in terms of one dominant factor. We have previously described LS_3 as a semirigid tridentate cavand-type ligand on the basis of molecular dynamics simulations and its structural chemistry.^{8b} Further, we have used this property to stabilize the cuboidal $[\text{Fe}_3\text{S}_4]^0$ unit, which decomposes in a less constraining ligand environment.¹³ Evidently, ligand “semirigidity” is not developed to the point where LS_3 cannot be detached from one cluster core and transferred to another, even in systems at ambient temperature lacking an exogenous nucleophile as a displacement agent.⁵⁵ The mechanism of ligand exchange is complicated and unclear.

Reaction systems **G–H** equilibrate in a matter of minutes, with the net result being the exchange of unidentate ligands between cluster cores in processes that are essentially statistical.

(54) Ciurli, S.; Holm, R. H. *Inorg. Chem.* **1989**, *28*, 1685.

(55) For example, LS_3 is readily removed from $[\text{Fe}_3\text{S}_4(\text{LS}_3)(\text{SET})]^{2-}$ by 3 equiv of NaSEt in Me_2SO to form $[\text{Fe}_4\text{S}_4(\text{SET})_4]^{2-}$ and $\text{Na}_3(\text{LS}_3)$ quantitatively *in situ*.¹³

Evidently, neither core has a dominant affinity for any one of ligands thiolate, chloride, cyanide, and phenolate. In a combinatorial experiment, cluster **2** was exposed to an equal deficiency (0.5 equiv) of benzenethiolate, phenolate, and cyanide in acetonitrile. The system initially containing 2^{Se} is shown in Figure 12. It is immediately apparent that 2^{Se} has been fully converted to a mixture of 3^{Se} , 8^{Se} , and 18^{Se} . Signal integration leads to the following affinity order: PhS^- (2.7) > PhO^- (1.7) > CN^- (1.0) \gg Cl^- . The same order and relative amounts were observed in the corresponding system based on 2^{S} . The affinity order, not determined previously, is fully consistent with numerous observations of ligand substitution, including those in the early development of the iron–sulfur cluster field.⁵⁶ It is a reaffirmation of the pronounced affinity of iron atoms in Fe_4Q_4 clusters for anionic sulfur ligands, a property that pervades all protein-bound iron–sulfur clusters of any type.

Summary. The following are the principal results and conclusions of this investigation:

1. [1:3] Site-differentiated $[\text{Fe}_4\text{Q}_4]^{2+}$ clusters ($\text{Q} = \text{S}, \text{Se}$) bind a wide variety of anionic and neutral mono-, bi-, and tridentate ligands L' at the unique site. Ligands include thiolates, phenolates, halides, cyclic triamines and trisulfides, imidazoles, and tertiary phosphines. The substituted cluster products $[\text{Fe}_4\text{Q}_4(\text{LS}_3)\text{L}']^{2-}$ are detectable by the isotropically shifted resonances of the LS_3 ligand, which are acutely sensitive to the nature of L' and without exception indicate trigonal symmetry in solution.

2. The non-halide clusters in (1) can be prepared by substitution of chloride in $[\text{Fe}_4\text{Q}_4(\text{LS}_3)\text{Cl}]^{2-}$. In general, thiolates and phenolates displace chloride stoichiometrically while an excess of most neutral ligands (in the presence of NaBF_4) is required.

3. In $[\text{Fe}_4\text{Q}_4]^{2+}$ clusters differing only in the core chalcogenide atom, isotropic shifts are larger (except for 2-H) and redox potentials are less negative when $\text{Q} = \text{Se}$. The larger shifts correlate with higher magnetic susceptibilities indicating reduced antiferromagnetic coupling. Redox potential differences typically are in the 20–60 mV interval except for the second reduction of $[\text{Fe}_4\text{Q}_4(\text{LS}_3)(\text{CN})]^{2-}$, for which the difference is 180 mV.

4. The crystal structure of $[\text{Fe}_4\text{Se}_4(\text{LS}_3)(\text{9}]\text{aneS}_3)]^-$ reveals idealized trigonal symmetry and demonstrates six-coordination at the unique Fe site. Bond distances suggest that the iron atom is biased toward the high-spin Fe(III) description.

5. With use of the clusters $[\text{Fe}_4\text{S}_4(\text{LS}_3)(\text{SET})]^{2-}$ (–1.11 V) and $[\text{Fe}_4\text{S}_4(\text{LS}_3)(4\text{-MeIm})]^-$ (–0.79 V), the intrinsic potential difference between protein-bound $[\text{Fe}_4\text{S}_4(\text{Cys-S})_4]^{2-}$ and $[\text{Fe}_4\text{S}_4(\text{Cys-S})_3(\text{His-N})]^-$ is estimated as 320 mV for the $[\text{Fe}_4\text{S}_4]^{2+,+}$ couple. The potential difference between two such clusters in *D. gigas* hydrogenase is 60 mV, suggesting some attenuation of the potential difference by protein environmental and pH effects. This enzyme is the only known case of imidazole binding to a native Fe_4S_4 center.

6. The tridentate LS_3 ligand undergoes slow exchange between $[\text{Fe}_4\text{S}_4]^{2+}$, $[\text{Fe}_4\text{Se}_4]^{2+}$, and $[\text{MoFe}_3\text{S}_4]^{3+}$ cores. The clusters $[\text{Fe}_4\text{S}_4(\text{LS}_3)\text{L}']^{2-}$ and $[\text{Fe}_4\text{Se}_4(\text{LS}_3)\text{L}'']^{2-}$ exchange ligands $\text{L}'/\text{L}'' = \text{EtS}^-, \text{Cl}^-, \text{CN}^-,$ and $p\text{-BrC}_6\text{H}_4\text{O}^-$. For both types of ligand exchange, equilibrium constants are near the statistical value of unity ($K_{\text{eq}} \approx 0.2\text{--}1.5$) in acetonitrile, suggesting that there is little differential affinity of the three cores for LS_3 binding and of the $[\text{Fe}_4\text{Q}_4]^{2+}$ cores for binding of these unidentate ligands.

(56) (a) Que, L., Jr.; Bobrik, M. A.; Ibers, J. A.; Holm, R. H. *J. Am. Chem. Soc.* **1974**, *96*, 4168. (b) Wong, G. B.; Bobrik, M. A.; Holm, R. H. *Inorg. Chem.* **1978**, *17*, 578.

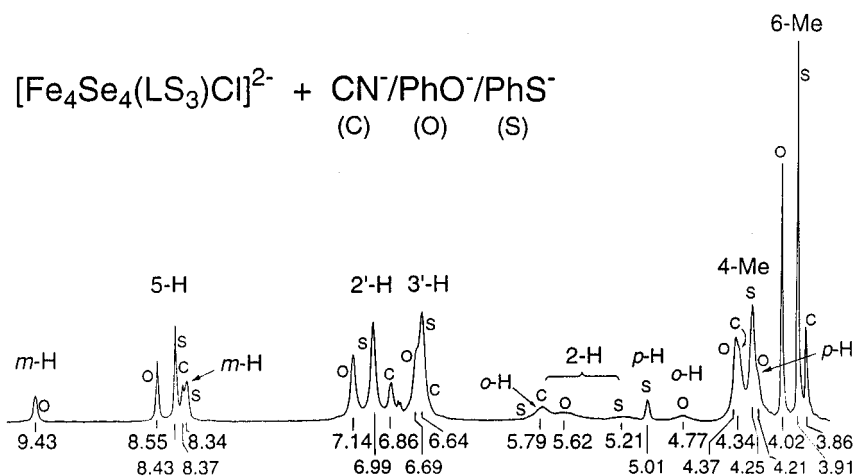


Figure 12. ^1H NMR spectra in acetonitrile solution (297 K) of the indicated ligand substitution system. Signals are designated as belonging to (c) cyanide-, (o) phenolate-, or (s) benzenethiolate-ligated clusters.

7. In competition experiments involving $[\text{Fe}_4\text{Q}_4(\text{LS}_3)\text{Cl}]^{2-}$ and selected added ligands, the affinity binding order $\text{PhS}^- > \text{PhO}^- > \text{CN}^- > \text{Cl}^-$ for $\text{Q} = \text{S}$ and Se was established in acetonitrile. Observation of these reactions and those in (6) depends entirely on the extreme sensitivity of LS_3 isotropic shifts to ligation at the unique iron site and to cluster spin state.

The results reported here constitute the most recent part of our study of the reactivity of iron–sulfur clusters in nonredox processes. When integrated with the findings of earlier investigations,^{10,11,14} a comprehensive picture of ligand binding to single iron sites in cubane-type $[\text{Fe}_4\text{Q}_4]^{2+}$ clusters emerges. Elsewhere, we have shown that cuboidal $[\text{Fe}_3\text{S}_4]^0$ clusters undergo metal ion incorporation reactions to afford heterometal cubane-type MFe_3S_4 clusters.⁵⁷

Acknowledgment. This research was supported by NIH Grant GM 28856. We are indebted to B. M. Segal for crystallographic experiments.

Supporting Information Available: X-ray structural information for the compound in Table 1, including tables of crystal and intensity data, positional and thermal parameters, and interatomic distances and angles (11 pages). Ordering information is given on any current masthead page.

IC970254U

(57) Zhou, J.; Raebiger, J. W.; Crawford, C. A.; Holm, R. H. *J. Am. Chem. Soc.* **1997**, *119*, 6242.